Wave-induced winds for shoaling waves: a laboratory study

Fabio Addona, Università di Parma, fabio.addona@unipr.it

INTRODUCTION

Air-sea fluxes of heat, gases, momentum is dominated by the interaction between air and water at the interface (Donelan, Csanady, 2001). It is intuitive that wind generates wave by exerting a stress on the surface. Several researchers focused on the energy and momentum transfer at the air-sea interface by parametrizing a drag coefficient to express wind-generated waves in terms of a single velocity in air (usually the air friction velocity u_* or the 10-m velocity U_{10}) (Sullivan and McWilliams, 2010). Many coupled ocean-atmosphere models rely on such parametrization for weather forecasting (Cavaleri et al, 2007), which often imply that wind velocity is higher than the wave phase speed. However, less attention has been devoted to swell propagating faster than the reference wind speed, which in the real world can appear both offshore and nearshore. In that case, the wave field generates (wave-induced) winds, and transfers momentum and energy to the atmosphere. Recent studies showed that the current models used for coupled models are not adequate to describe this phenomenon, yielding to misleading forecasting (Smemdan 1999, CBLAST-Low, Yun and French 2016, Aird et al. 2022). Here, we present a laboratory study of a monochromatic wave propagating on a mild-slope bottom, in conditions of no wind. Our aim is to observe how different wave frequencies and water depths influence the air flow above.

EXPERIMENTS AND METHODS

Experiments were taken at the wind-wave tank located at the University of Delaware. The facility is 42-m-long, 1-m-wide and 1.25-m-high. A plunger-type wave maker was used to generate wave. For this set of experiments, the wind tunnel was kept off since we wanted to observe the wave-driven winds and turbulence. We inserted a mild-slope bottom with two decremental slope angles to generate wave shoaling. At the measurements section, the bottom was flat. To avoid wave reflection, we used one more inclined ramp after the flat section (which avoid bottom steps) and an absorbing beach at the end of the tank. See figure 1 for a sketch of the experimental apparatus.

We used a combination of PIV (Particle Image Velocimetry) and PLIF (Particle Laser Induced Fluorescence) to measure the free surface and the 2D

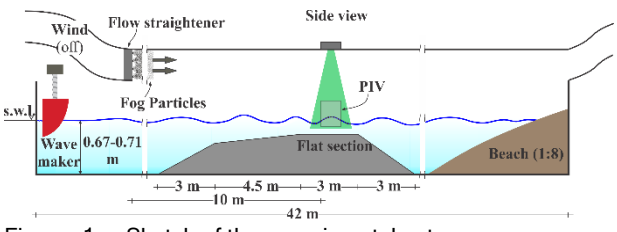

Figure 1 - Sketch of the experimental set-up

velocity field in air. The system consisted of three cameras: one used for PIV measures and two for PLIF measures. The advantage of using 2 PLIF cameras is to have one with a smaller Field of View (FoV) for a better resolution of the free surface, and one with a bigger FoV to capture the longer components of the shoaling wave. The camera system is illustrated in Figure 2.

We generated fog particles in air with a diameter of 10 um as tracers for PIV, and Rhodamine in water for PLIF. The PIV system acquired at 29 Hz (14.5 Hz each image couple) and was processed with a pyramidal cascade of interrogation windows to increase the dynamical range of the measured velocity. We used a combination of PIV (Particle Image Velocimetry) and PLIF (Particle Laser Induced Fluorescence) to measure the free surface and the 2D We adopted a particular protocol to measure air velocity. Since we did not want the measurements to be contaminated by the fog velocity, we generated fog for 5 minutes before the test. Then, we waited two minutes before starting the wave maker to generate the shoaling waves.

For this activity, we tested two values of the wave amplitude (a_{rms} = 1.4 - 2.4 cm) and two values of water depth (h = 0.04-0.08 m in the measurements section), for a total of 4 experiments. The wave frequency f = 1.45 Hz was kept the same for all the tests.

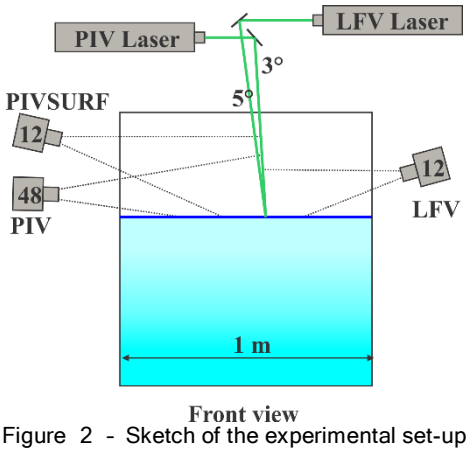

Figure 2 - Sketch of the experimental set-up

RESULTS

So far, we have focused our study on the instantaneous air velocity field. If we take a look to the horizontal velocity, we observe that, for the same water depth (h = 0.08 m), the smaller wave height (a_{rms} = 2.4 m, see Figure 3) gives a horizontal velocity field which follows the potential theory over the crest. However, a modest dragged wave-induced wind can already be seen after the crest passes (the wave moves from left to right). The situation is remarkably changed in Figure 4, where we consider the same water depth and an increased wave height (a_{rms} = 2.4 m). For this second case, the wave-induced air flow is significant way above the crest of the wave for almost all the wave length, with the exception of the crest areas, where the orbital velocity is still significant.

These results are preliminary and have the only aim to briefly show the complex air pattern produced by shoaling waves (in the absence of wind). The next steps will be to study the 2D velocity field through a triple decomposition and to separate the momentum and energy contributions of the mean, of the orbital and of the turbulent components.

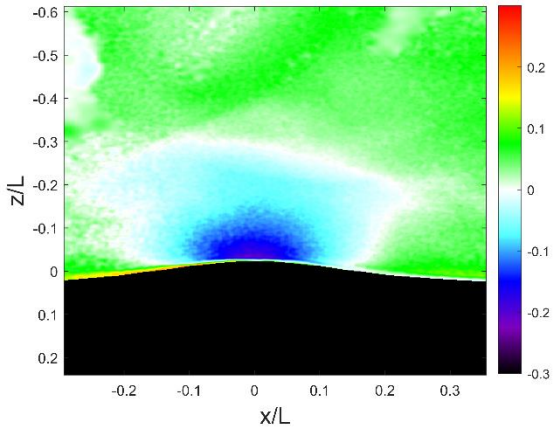

Figure 3 - Instantaneous horizontal velocity for shoaling wave (a_{rms} = 1.4 m, f = 1.45 Hz) with water depth h = 0.08 m. L is the wave length computed from the linear dispersion relation; z = 0 is the mean water level, while x = 0 is the position of the crest.

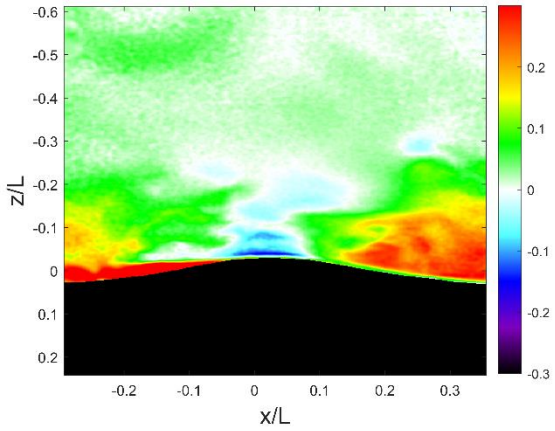

Figure 2 - Instantaneous horizontal velocity for shoaling wave (a_{rms} = 2.4 m, f = 1.45 Hz) with water depth h = 0.08 m. L is the wave length computed from the linear dispersion relation; z = 0 is the mean water level, while x = 0 is the position of the crest.

REFERENCES

Aird, Barthelmie, Shepherd, Pryor (2022). Occurrence of Low-Level Jets over the Eastern U.S. Coastal Zone at Heights Relevant to Wind Energy *Energies* 15, no. 2: 445.

Cavaleri, Alves, Ardhuin, Babanin, Banner, Belibassakis, ... and WISE Group. (2007). Wave modelling-the state of the art. Progress in oceanography, 75(4), 603-674.

Csanady. (2001). Air-sea interaction: laws and mechanisms. Cambridge University Press.

Donelan, M. A. (1990). Air-sea interaction.

Edson, Crawford, Crescenti, … , ZappaThe coupled boundary layers and air-sea transfer experiment in low winds. Bulletin of the American Meteorological Society, 88(3), 341-356.

Smedman, Högström, Bergström, Rutgersson, Kahma, Pettersson (1999). A case study of air-sea interaction during swell conditions. Journal of Geophysical Research: Oceans, 104(C11), 25833-25851.

Sullivan, P. P., & McWilliams, J. C. (2010). Dynamics of winds and currents coupled to surface waves. Annual Review of Fluid Mechanics, 42, 19-42.

Sun, French (2016): Air-sea interactions in light of new understanding of air-land interactions. Journal of the Atmospheric Sciences, 73(10), 3931-3949.